Separation Science and Technology
Publication details, including instructions for authors and subscription information:
http://www.informaworld.com/smpp/title~content=t713708471

Separation of Fine Particles from Nonaqueous Media: Free Energy Analysis and Oil Loss Estimation

V. B. Menon[ab]; R. Nagarajan[a]; D. T. Wasan[a]
[a] Department of Chemical, Engineefjng Illinois Institute of Technology, Chicago, Illinois [b] Research Triangle Institute, North Carolina

To cite this Article Menon, V. B. , Nagarajan, R. and Wasan, D. T.(1987) 'Separation of Fine Particles from Nonaqueous Media: Free Energy Analysis and Oil Loss Estimation', Separation Science and Technology, 22: 12, 2295 — 2322
To link to this Article: DOI: 10.1080/01496398708057188
URL: http://dx.doi.org/10.1080/01496398708057188

SEPARATION SCIENCE AND TECHNOLOGY, 22(12), pp. 2295-2322, 1987

Separation of Fine Particles from Nonaqueous Media: Free Energy Analysis and Oil Loss Estimation

V. B. MENON,* R. NAGARAJAN, and D. T. WASAN

DEPARTMENT OF CHEMICAL ENGINEERING
ILLINOIS INSTITUTE OF TECHNOLOGY
CHICAGO, ILLINOIS 60616

Abstract

In industrial processes for the separation of fine particles from oil to produce clean liquid fuels, a significant portion of oil is entrained by the solids and is lost. A semi-empirical model is proposed to explain the mechanism of oil loss and floc carryunder. The favorability of the transfer of fine particles from oil to water was determined by conducting a free energy analysis of the process. The ratio of the water drop to particle radius (size ratio) and the contact angle were found to be important parameters affecting the free energy change. The oil loss was found to increase with an increase in size ratio. To verify the model, experiments to determine oil loss in a practical system were conducted for two different surfactants. The model was found to fit experimental data for oil loss very well. The results show that by choosing a suitable surfactant and demulsifier, it is possible to decrease the oil loss considerably. Hence, the proposed model is useful for evaluating the efficiency of the separation process.

INTRODUCTION

During the production of petroleum and synthetic liquid fuels from shale, coal, and tar sands, fine mineral particles get dispersed in the oil. This necessitates the cleaning of the oil prior to further processing. Fine particles contribute to fouling, coking, erosion, foaming, and other problems in downstream processing units. Conventional means of

*Current address: Research Triangle Institute, P.O. Box 12194, Research Triangle Park, North Carolina 27709.

particle removal such as filtration, centrifugation, and sedimentation are not economical owing to the large volumes of oil that have to be treated. One method that is frequently used in such industries is known as "dedusting." Figure 1 is a schematic of such a process (*1*). The removal of particles is accomplished by dispersing water into the oil in the presence of surfactants, forming a solids-stabilized water-in-oil emulsion. The emulsion, with particles arranged on the drop surfaces, has to be demulsified in a settler before clean oil can be recovered. The solids-stabilized emulsions which result from a dedusting operation are, however, very stable and their coalescence involves considerable expense. The emulsions form a sludge layer in the settler, resulting in oil loss due to entrainment. This oil loss can be as high as 5–6 g oil/g solids. A model for estimating oil loss for a given surfactant–demulsifier mixture can be very useful in evaluating the performance of various chemicals in demulsification operations. A part of the sludge layer often decomposes into flocs which break through the bulk oil/water (O/W) interface and settle to the bottom of the settler. This phenomena of floc carryunder is favorable because it decreases the volume of sludge that has to be treated and disposed.

This paper reports the results of our investigation of the thermodynamic analysis of particle transfer from oil to water and of the

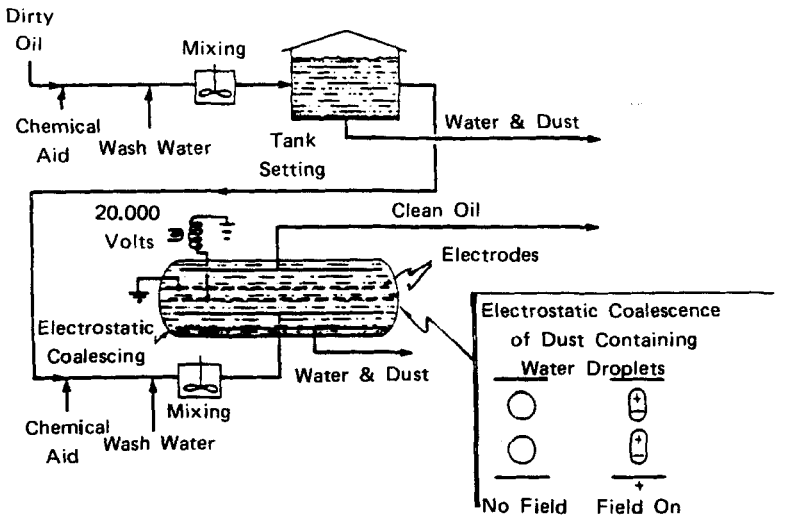

FIG. 1. Schematic of the dedusting process for separation of particles from oil [from Kaye and Fiocco (*1*)].

phenomenon of oil loss and floc carryunder. The thermodynamic free energy analysis is aimed at determining the role of different variables in determining the ease of emulsion formation and its subsequent stability. The oil loss model enables the determination of the extent of oil entrainment for a particular surfactant/demulsifier mixture provided that the oil/water interfacial tension and the three-phase contact angle are known. Since interfacial tension and contact angle are fundamental properties that can be easily measured, this model is suitable for comparing the oil losses that can be expected with different surfactants and demulsifiers.

EXPERIMENTAL

The solid phase consisted of shale dust particles supplied by Exxon Research and Engineering Company (ER&E Co.). The particles had an average diameter of 4 μm. The oil phase was a 1:1 volume mixture of heptane and toluene which we shall henceforth call "heptol." The surfactants studied were Aerosol-OT, obtained from American Cyanamid Co., and Pluronic P-103, supplied by ER&E Co. The demulsifier blend of Breaxit-126 (BR-126) and Corexit-420 (CR-420) were supplied by ER&E Co. BR-126 is a mixture of oxyalkylated phenolic resins in glycol ether and aromatic solvents. CR-420 is a blend of ester surfactant and aryl sulfonic acid in mixed aromatic solvents.

Two sets of experiments, each with a different surfactant, were conducted. The procedure for all the experiments was identical and is outlined. The oil phase was prepared by mixing 5 g of spent shale dust with 73 g heptol. A known weight of the surfactant was added to this dispersion. Double distilled water (25 mL) was added to the oil phase along with 0.02 g of the demulsifier, Breaxit-126. The mixture was stirred at a fixed speed for 30 min using a magnetic stirrer. The agitation produced a solids-stabilized emulsion. In all the experiments, the stirrer geometry, the speed of agitation, the temperature, and the volume fraction of water and solid were kept the same. The only variable that was changed systematically was the surfactant concentration. Once the emulsion was prepared, it was transferred to a separatory funnel and allowed to settle for 24 h. After this period the emulsion separated into a clear upper oil phase and a blackish lower phase containing the solids. Owing to the dark color of the solids, it was not possible to discern the existence of a sludge layer. The presence of solids in the bottom water phase clearly indicates that part of the sludge layer must have formed

flocs which broke through the O/W interface and settled into the separated water phase.

About 45 cm^3 of the solids-rich water from the bottom of the separatory funnel was withdrawn and centrifuged at 1500 rpm for 15 min. The volumes of the gel (bottom), water (middle), and oil (top) phases in the tube were accurately recorded. After decanting the oil and water from the centrifuge tubes, the remaining gel was weighed. The water content of the gel was then determined by distillation as specified by ASTM Standard Test Method D95. In this method the gel, along with 30 cm^3 of toluene, was heated under reflux in a flask. Toluene and water codistilled, and was condensed and collected in a Dean Stark trap, with the water settling in the graduated section of the trap and the toluene returning to the flask. After distilling for 3 h, the volume of water in the trap was recorded. The solids were removed from the flask, dried, and weighed. From a material balance it was then possible to determine the amounts of solids, oil, and water in the gel. The oil loss was expressed as the weight of oil lost per unit weight of solids. The detailed procedure for determining oil loss has been described elsewhere (*2*).

Prior to the oil loss determination, samples of the clear oil, water, and solids were extracted from the separatory funnel and used to determine the interfacial tension and the contact angle for the different concentrations of the surfactant that were studied. The interfacial tension was measured using a spinning drop tensiometer. The contact angle was measured by the goniometric method, using a flat disk of the particles prepared at 35,000 lb in a potassium bromide die.

Two surfactants, Aerosol-OT and Pluronic P-103, were used to evaluate the validity of the oil loss model. The first surfactant was used to estimate the parameters of the oil loss equation and the second surfactant was used to verify the applicability of the equation for different surfactants.

FREE ENERGY ANALYSIS

The transfer of a single particle from oil to the interior of a water droplet is one example where the transfer can be viewed simply from a thermodynamic viewpoint in which only the initial and final energy states are considered. Such an analysis was conducted by Jacques et al. (*3*) for the transport of a single spherical particle into a water droplet while both are suspended in oil. Their analysis revealed that only hydrophilic particles, i.e., only particles with a contact angle less than 90°, could exist within the water droplet. Also, the ratio of the size of the water

drop to that of the particle was found to be important in determining the ease of the transfer process.

In real systems the particles collect at the interface between the water drop and the continuous oil phase (Fig. 2). Rapachietta and Neumann (*4*) analyzed the free energy change when a solid sphere finds its equilibrium position at an infinitely flat O/W interface. A free body force analysis has also been conducted by a number of investigators to find the equilibrium position of a solid sphere at a planar interface. From such a force balance the critical size of the particle beyond which equilibrium at the interface is impossible has been derived (*4*, *5*). The aforementioned analyses have been restricted to a single particle-planar interface system. Actual systems involve a large ensemble of particles collected at curved drop-liquid interfaces. It was therefore found relevant to conduct a free-energy analysis of the process of particle transfer from oil to a water drop

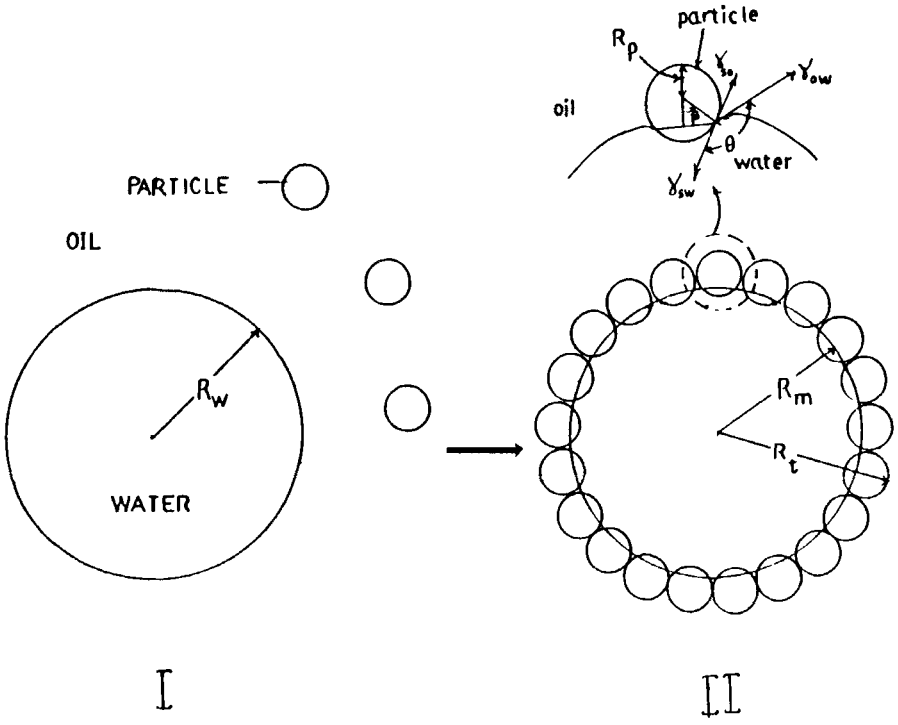

FIG. 2. Schematic of the mechanism of particle transfer from oil to a water drop.

incorporating the effects of many particles as well as curvature of the interface.

Figure 2 depicts the mechanism of particle transfer from oil to a water drop. "I" refers to the initial state and "II" refers to the final state. It is desired to find the conditions and relevant parameters which favor State II over State I. The schematic shown in this figure is the most prevalent mode of particle transfer that has been experimentally observed and results in the formation of solids-stabilized emulsions.

R_w is the radius of the water drop and R_p is the particle radius. Neglecting the effects of gravity, the free energy of State I can be written as

$$F_{\mathrm{I}} = 4\pi R_w^2 \gamma_{ow} + N_p 4\pi R_p^2 \gamma_{so} \tag{1}$$

where N_p is the number of particles available to a water drop and γ_{ow} and γ_{so} are the oil/water and solid/oil interfacial tensions, respectively.

The free energy of State II is

$$F_{\mathrm{II}} = (4\pi R_m^2 - N_p \pi R_p^2 \sin^2 \beta)\gamma_{ow} + N_p 2\pi R_p^2 (1 - \cos \beta)\gamma_{sw} + N_p 2\pi R_p^2 (1 + \cos \beta)\gamma_{so} \tag{2}$$

where R_m is the new radius of the water drop when the particles are present at the interface, and β is the angular position of the particles on the water drop (see Fig. 2).

R_m can be obtained from a volume balance:

$$\frac{4}{3}\pi R_m^3 = \frac{4}{3}\pi R_w^3 + N_p\left[\frac{\pi R_p^3}{3}(1 - \cos \beta)^2(2 + \cos \beta)\right] \tag{3}$$

or

$$R_m^3 = R_w^3 + \frac{N_p}{4} R_p^3 (1 - \cos \beta)^2 (2 + \cos \beta) \tag{4}$$

The free energy change from State I to State II is the difference between Eqs. (1) and (2):

$$F_{\mathrm{II}} - F_{\mathrm{I}} = (4\pi R_m^2 - 4\pi R_w^2 - N_p \pi R_p^2 \sin^2 \beta)\gamma_{ow} + (N_p 2\pi R_p^2)(\gamma_{sw} - \gamma_{so})(1 - \cos \beta) \tag{5}$$

The interfacial tensions are related to each other by Young's equation, which can be written as:

$$\gamma_{so} - \gamma_{sw} = \gamma_{ow} \cos \theta \tag{6}$$

where θ is the three-phase contact angle measured through the water phase (θ is 0° for a completely hydrophilic solid and 180° for a completely hydrophobic solid).

The free energy change per unit surface area of the particle per unit O/W interfacial tension is

$$\Delta F = \left[\frac{R_m^2 - R_w^2}{R_p^2}\right] - \frac{N_p}{4} \sin^2 \beta - \frac{N_p}{2} \cos \theta (1 - \cos \beta) \tag{7}$$

The ratio of the drop radius to the particle radius can be termed **n**. Hence,

$$\mathbf{n} = R_w / R_p$$

Therefore,

$$\Delta F = \left[\mathbf{n}^3 + \frac{N_p}{4}(1 - \cos \beta)^2 (2 + \cos \beta)\right]^{2/3} - \mathbf{n}^2 - \frac{N_p}{4} \sin^2 \beta - \frac{N_p}{2} \cos \theta (1 - \cos \beta) \tag{8}$$

From the above equation it is evident that the free energy change, ΔF, is a function of the drop to particle size ratio (**n**), the number of particles per drop (N_p), the contact angle (θ), and the position parameter (β). If the water drop is completely covered with particles in an ordered hexagonal-close packed arrangement, then this represents the maximum number of particles that can exist on the drop surface. This number ($N_{p_{hex}}$) can be related to the other parameters by

$$N_{p_{hex}} = \frac{2\pi}{\sqrt{3}} \left(\frac{R_m + R_p \cos \beta}{R_p}\right)^2 \tag{9}$$

This equation must be simultaneously solved with Eq. (4) to obtain $N_{p_{hex}}$ as a function of **n** and β. A Newton-Raphson numerical scheme was used to solve for $N_{p_{hex}}$.

For State II to be favored over State I, ΔF must be negative. ΔF was therefore evaluated for various values of **n**, N_p, θ, and β, in order to ascertain the influence of these parameters on the stability.

Figure 3 shows the variation of ΔF with the three-phase contact angle for $\beta = 150°$ and different values of **n**. Hexagonal packing of particles on the drop surface was assumed. Note that the two ordinates of Fig. 3 have different scales. This figure reveals that the stability of State II decreases as θ increases (i.e., as the particle becomes more hydrophobic) and beyond a contact angle of 90°, ΔF becomes positive. The influence of **n** on the stability of State II over State I is considerable. As **n** is varied from 10 to 100, ΔF becomes more negative. The value of β chosen was arbitrary. However, in actuality, if the presence of the solid particle at the O/W interface does not deform the interface significantly, then

$$\beta \approx (180 - \theta) \tag{10}$$

This equation is generally true for large values of **n**.

For the spent shale dust/water/heptol system, θ is about 150°. If Eq. (10)

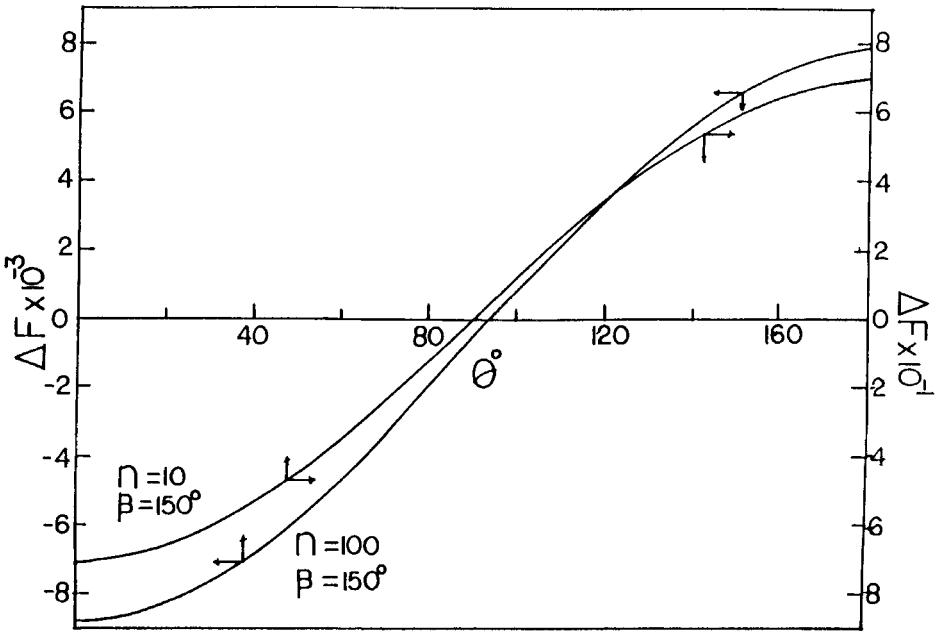

FIG. 3. Effect of contact angle on the free energy change for different **n** and $\beta = 150°$.

is assumed to hold, then $\beta \approx 30°$. Figure 4 shows the free energy change for two different values of $\mathbf{n}$ and $\beta = 30°$. A contact angle of 150° does give a negative value of ΔF, implying that particle transfer is favored. However, since the ΔF is close to zero, the stability of State II over State I is not very large. Hence, some redispersion of the particles back into the bulk oil would seem to be inevitable. This may be prevented by improving the wetability (decreasing θ) and/or increasing the value of $\mathbf{n}$.

From Figs. 3 and 4 it is seen that there exists a critical value of the contact angle (θ_{crit}) at which ΔF is zero. Contact angles above θ_{crit} do not give a stable situation for a particular value of β and $\mathbf{n}$. Figure 5 shows the influence of $\mathbf{n}$ on θ_{crit}. At large values of $\mathbf{n}$, θ_{crit} is almost independent of $\mathbf{n}$, but at low values of $\mathbf{n}$, the critical contact angle decreases sharply. This is especially true for low values of β. The region below each curve represents the permissible values of θ for any $\mathbf{n}$. This figure once again emphasizes the importance of $\mathbf{n}$ in determining the stability of State II vis-á-vis State I.

Figure 6 depicts the variation of ΔF with N_p, the number of particles on

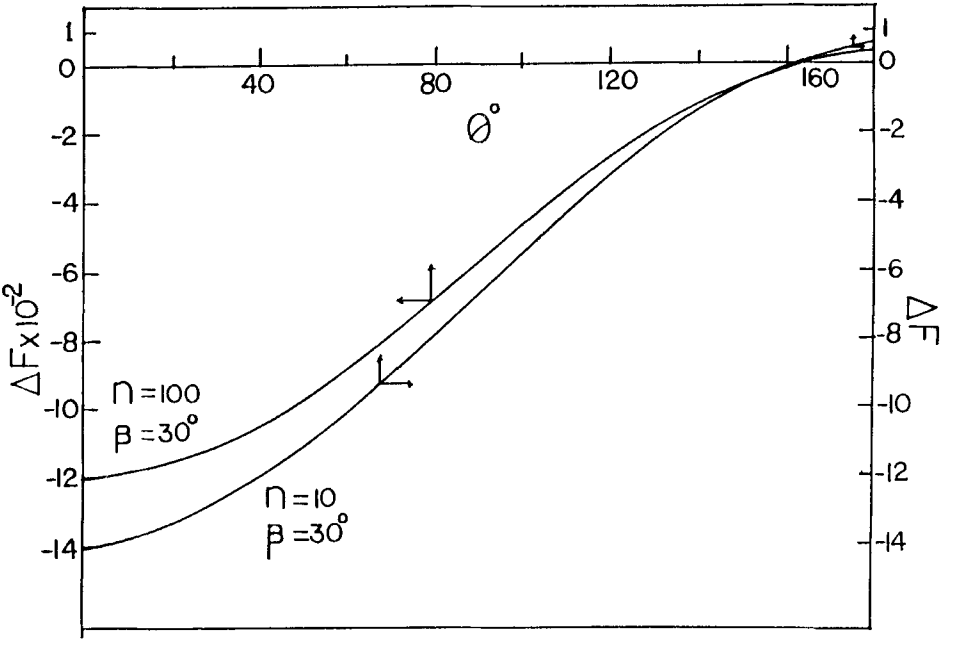

FIG. 4. Effect of contact angle on the free energy change for different $\mathbf{n}$ and $\beta = 30°$.

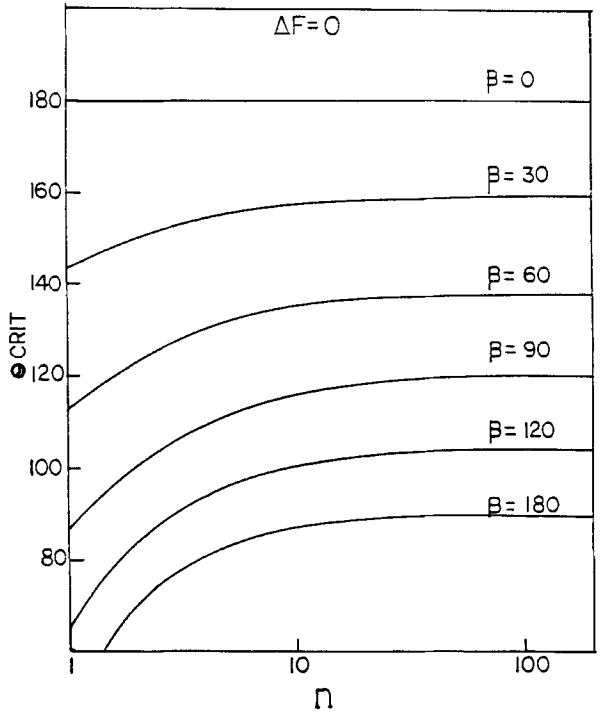

FIG. 5. Effect of **n** on the critical contact angle.

the drop. β has been arbitrarily set at 30°. For θ up to 150°, the increase of N_p increases the stability of State II, with a steeper increase for lower values of θ. For spent shale dust ($\beta \approx 30°$ and $\theta \approx 150°$) the increase in stability becomes significant only at N_p values greater than 1000.0. Of course, the maximum value of N_p that is permissible will be limited by N_{Phex} which is related to **n**. The system with $\beta = 30°$ and $\theta = 160°$ is unstable because θ is greater than θ_{crit}.

The above analysis reveals that higher values of **n** and N_p favor a more facile transfer of particles from oil to water. The system selection should also take into account the critical contact angle permissible for a given set of conditions.

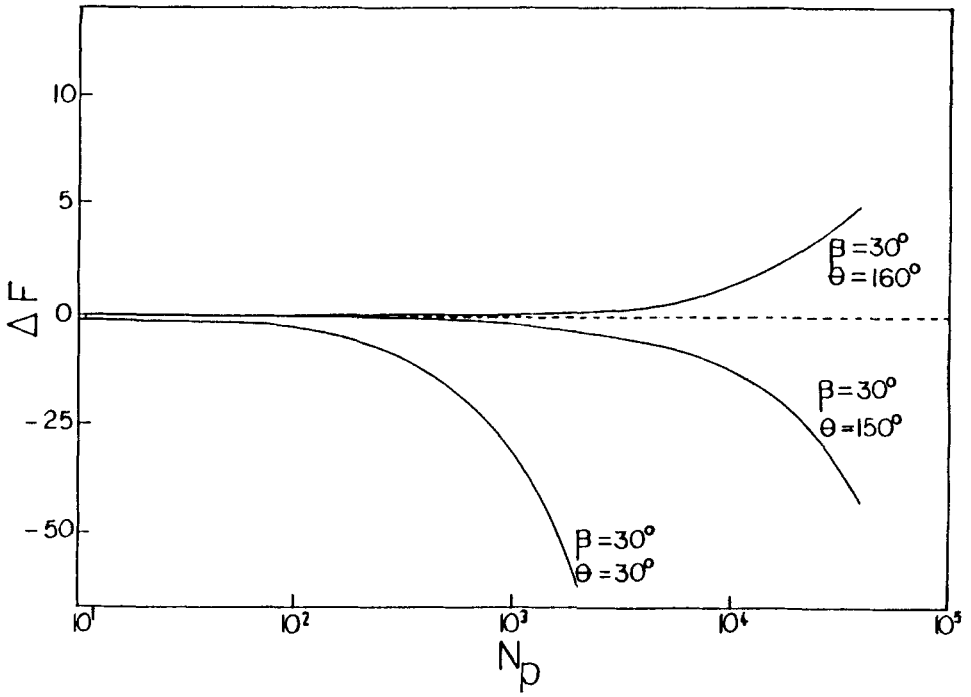

FIG. 6. Influence of the number of particles on the free energy change.

OIL LOSS ESTIMATION

Since the distribution of particles at the O/W interface is thermodynamically favored, the transfer process results in the formation of solids-stabilized water-in-oil emulsions. In a commercial unit the particle transfer is usually achieved in a mixer while the separation of the solids-stabilized emulsion is accomplished in the coalescer (or settler or electrocoalescer). Figure 1 is a simple schematic of the process. While some breakage of the emulsion is achieved in the coalescer through the use of demulsifiers and electric fields, a great portion of the emulsion droplets just settle to the O/W interface in the coalescer and form a sludge layer. A typical coalescer has three zones: (i) a clear upper oil layer where the concentration of emulsion droplets is low, (ii) a sludge layer where the emulsion droplets are densely packed, and (iii) a clear water layer at the bottom.

In an ideal coalescer unit, one desires complete coalescence of the

emulsions so that a clear upper oil phase and a clear lower water phase are obtained. The sludge layer is hence an undesirable third region which has to be removed to obtain clean oil. This is usually achieved by periodically skimming off the sludge layer by mechanical means. However, the sludge layer carries within it a significant amount of entrained oil, and discarding of the sludge layer involves the loss of this oil. The oil loss is usually expressed in weight of oil lost per unit weight of solids. Then large volumes of oil are to be treated, it becomes economically imperative to find the mechanism of oil loss and determine the variables that affect it. Subsequently, ways can be devised to reduce the oil loss.

In this section, a model for oil loss is proposed. Experiments were conducted to measure the oil loss and the results were correlated with the model.

Figure 7 depicts the sludge layer that is formed in the settler when uncoalesced emulsion droplets settle to the top of the separated water phase. Oil loss occurs due to the entrainment of oil in the voids between emulsion droplets in the sludge layer (V_{ou} in Fig. 7) and in the interstices between particles on each water drop (V_{os} in Fig. 7).

Calculation of V_{ou}. The solids-stabilized water drops can be assumed to be arranged in a simple cubic packing arrangement in the sludge layer. This assumption was made since our objective was to determine the maximum possible oil loss. This is the hard sphere model approximation.

$$\text{Void volume in sludge} = (1 - \pi/6)V \tag{11}$$

where V is the total volume in the sludge layer.

$$\text{Volume occupied by emulsion droplets} = \pi/6V \tag{12}$$

On each drop, the solids can be assumed to be in a hexagonal close-packed arrangement. This is the same assumption that was made in calculating the free energies in the previous section. Equation (9) then gives the number of particles per drop.

V_{ou} is defined as the ratio of the weight of oil in the voids of the sludge to the weight of solids in the sludge.

$$V_{ou} = \frac{(1 - \pi/6)V}{\pi/6V} \frac{\rho_o}{\rho_p} \frac{1}{N_p} \frac{1}{R_p^3/R_t^3} \tag{13}$$

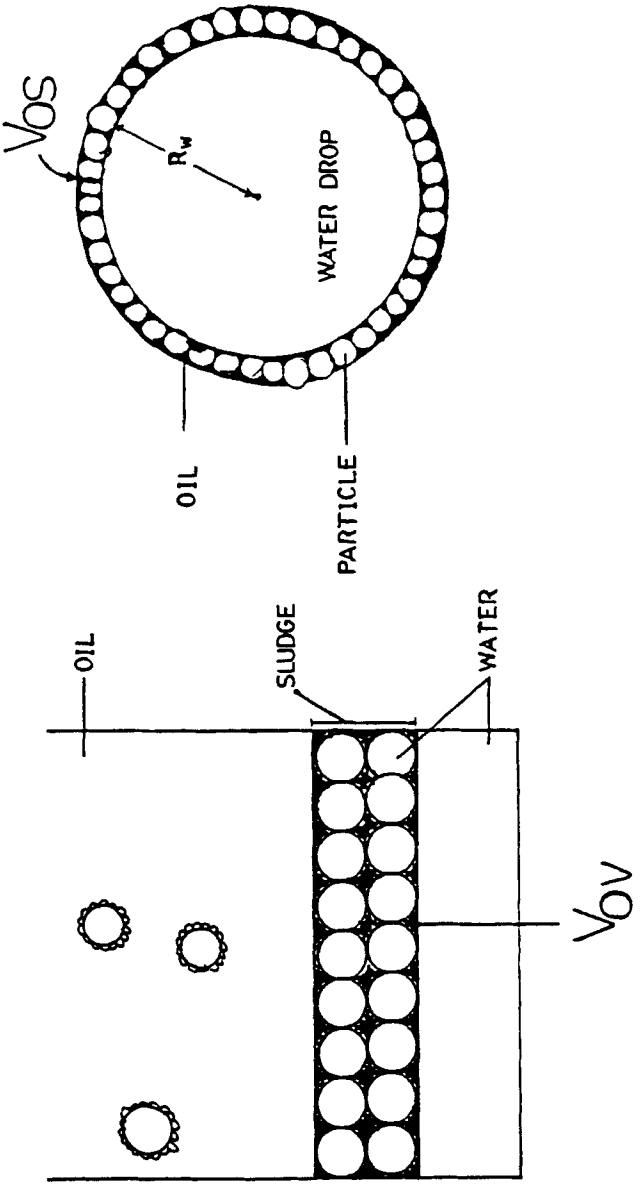

FIG. 7. Schematic of the sludge layer (left) and the packing of particles on a water drop (right).

ρ_o and ρ_p are the densities of oil and solid, respectively, and R_t is given by

$$R_t = R_w + R_p(1 + \cos\beta) \tag{14}$$

The water drop radius being much larger than the particle radius, the change in R_w is negligible and $R_m \approx R_w$. Thus,

$$V_{ov} = 0.2508 \frac{\rho_o}{\rho_p} \frac{(\mathbf{n} + \cos\beta + 1)^3}{(\mathbf{n} + \cos\beta)^2} \tag{15}$$

Calculation of V_{os}. V_{os} is defined as the ratio of the weight of oil in the interstices to the weight of solids per drop:

$$V_{os} = \frac{\rho_o}{\rho_p} \frac{(4\pi/3R_t^3 - N_p V_{sp} - 4\pi/3R_w^3)}{(4\pi/3N_p R_p^3)} \tag{16}$$

where V_{sp} is the volume of each particle above the oil/water interface and can be written as

$$V_{sp} = \frac{\pi R_p^3}{3}[4 - (1 - \cos\beta)^2(2 + \cos\beta)] \tag{17}$$

V_{os} can be obtained from Eqs. (16) and (17). It turns out that V_{os} is dependent only on the size ratio, **n**, and not on their absolute values. Also,

$$V_{tot} = V_{os} + V_{ov} \tag{18}$$

In order to compute V_{tot} we further need to assume that $\beta \approx (180 - \theta)$. In Fig. 8 the variation of V_{tot} is shown with **n** for two different values of θ. The oil loss increases with an increase in **n**. The influence of the contact angle on the oil loss is not significant since the plots shift very little with large changes in contact angle. Figure 8 also shows the importance of **n** on the oil loss. In an earlier section we found that the ease of particle transfer from oil to water increases with increasing **n**. Here we find that oil loss also increases with increasing **n**. Hence, the lower the oil loss, the more difficult the process of particle transfer. A judicious choice of **n** is therefore absolutely essential to reduce oil loss as well as have a reasonably favorable capture efficiency of particles by water droplets.

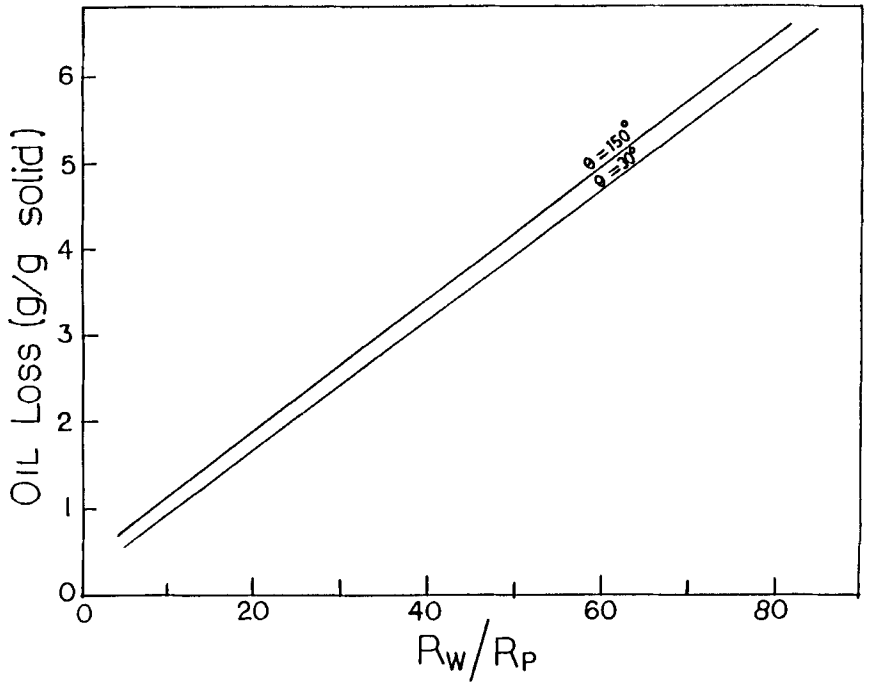

FIG. 8. Variation of oil loss with size ratio (**n**).

The individual contributions of V_{ov} and V_{os} to the oil loss are shown in Table 1 for $\theta = 150°$. The oil loss, V_{os}, is less than 8% of the total oil lost.

Since the oil loss expression is in terms of **n**, θ, and the density ratio of oil and water, one would need to know the size ratio for a particular system before oil loss could be calculated. In actual practice the determination of drop sizes is not easy since the emulsion is usually prepared in an agitated vessel. It is therefore of great use if **n** can be expressed in terms of known parameters such as the oil/water interfacial tension and the contact angle. The rest of this section is aimed at reducing the oil loss equation to an expression containing the O/W interfacial tension and the contact angle.

In agitated vessels the drop size of the dispersion can be related to the agitator speed, volume fraction, interfacial tension, density difference, and impeller dimensions by semi-empirical equations. If, for a system, all variables excepting the interfacial tension are maintained constant, then

TABLE 1
Comparison of the Contributions of V_{ov} and V_{os} to the Total Oil Loss at Various Size Ratios and $\theta = 150°$

n	V_{os}	V_{ov}	V_{tot}
10	0.0978	1.0634	1.1612
20	0.1284	1.8045	1.9329
30	0.1402	2.5524	2.6926
40	0.1465	3.3021	3.4486
50	0.1504	4.0525	4.2029
60	0.1529	4.8032	4.9561
70	0.1549	5.5542	5.7091
80	0.1563	6.3053	6.4616
90	0.1575	7.0565	7.2140
100	0.1584	7.8078	7.9662

$$R_w = f(\gamma_{ow}) \tag{19}$$

The functionality commonly used is

$$R_w = K_1 \gamma_{ow}^{\alpha} \tag{20}$$

where K_1 and α are constants. Since R_p is usually fixed for a system,

$$R_w/R_p = \mathbf{n} = K_2 \gamma_{ow}^{\alpha} \tag{21}$$

where K_2 is a new constant. It should be noted that the constant K_2 contains within it the dependence of drop size on all the variables other than O/W interfacial tension. The substitution of this form of equation for **n** in the oil loss equation now enables one to estimate oil loss from a knowledge of the interfacial tension. The constants K_2 and α need to be determined from experimental data. The advantage of an equation of oil loss in terms of γ_{ow} and θ is that various surfactants can be evaluated to find the one which gives the lowest oil loss.

The final expression for oil loss in terms of γ_{ow}, θ, K_2, and α is

$$V_{tot} = 0.2508 \frac{\rho_o}{\rho_p} \frac{(K_2 \gamma_{ow}^{\alpha} + 1 - \cos\theta)^3}{(K_2 \gamma_{ow}^{\alpha} - \cos\theta)^2} \tag{22}$$

where it has been assumed that $\beta = (180 - \theta)$ and that the contribution of V_{os} to the total oil loss is negligible. The above expression for oil loss assumes that particles are always in a hexagonally close-packed arrange-

ment on each drop surface. However, since a change in interfacial tension would involve a change in drop size and since the solids concentration has been treated to be invariant, it means that as the drop size changes there will be some solids concentrations where the number of particles is less or more than that required for hexagonal packing. Our experiments were conducted with a constant solids concentration which was always in excess of that required for hexagonal packing. The oil loss associated with particles in excess of hexagonal packing is negligible provided that they are not flocculated in the bulk oil phase. Our analysis does not take into account any flocculation that may occur in oil, and the oil loss associated with such a phenomenon has not been considered. It has also been assumed that the agitation vessel, speed of agitation, density difference, and volume fraction of the dispersed phase are all maintained constant.

Experiments were conducted to check the model with experimental data and find the value of the two parameters K_2 and α. Since the model indicates a direct dependence on γ_{ow} and θ, the experiments involved the use of surfactants such as Aerosol-OT, Pluronic P-103, and Breaxit-126 (demulsifier) with which γ_{ow} and α could be changed systematically and oil loss estimated.

Figure 9 shows the effect of the two surfactants on the interfacial tension. The abscissa depicts the initial concentration of surfactant that was added to the oil. The interfacial tension was measured using the spinning drop tensiometer for the phases in equilibrium with each other. The interfacial tension decreases with increasing surfactant concentration and attains its critical micelle concentration around 500 ppm. Similar behavior is exhibited by Pluronic P-103 but with larger values of the interfacial tension. Figure 10 shows the effect of surfactant on the equilibrium three-phase contact angle measured through the water phase. The contact angle does not appear to be affected by the presence of the surfactant.

Figure 11 shows the variation of oil loss with increasing surfactant concentration. The data points are experimental measurements of the oil loss while the line represents the calculation of oil loss from the geometric model using the interfacial tension and contact angle values shown in Figs. 9 and 10. The two parameters K_2 and α determined for Aerosol-OT were found to be 20.2 and 0.44, respectively. These two parameters will remain unchanged as long as all the variables other than interfacial tension and contact angle are fixed. This was indeed the case for Pluronic P-103 as the surfactant. Using the above values of K_2 and α, and the interfacial tension and contact angle from the experiments (Figs. 9 and 10), the oil loss was calculated as a function of surfactant

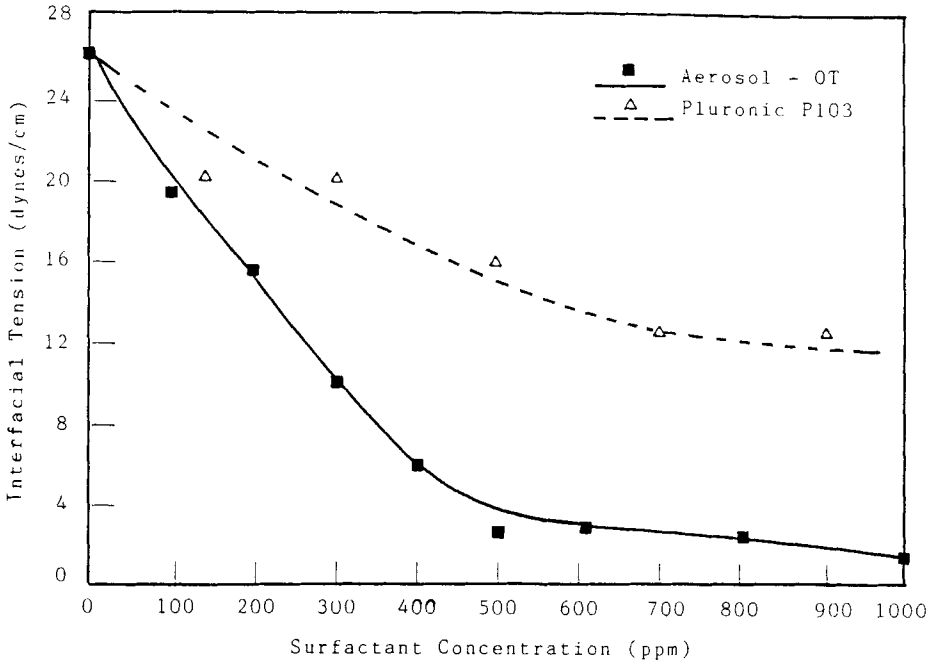

FIG. 9. Effect of surfactant on interfacial tension.

concentration from Eq. (22) and is plotted in Fig. 11. It is evident that the geometric model is able to account very well for the oil loss behavior. Thus, such a model can be used to evaluate the efficiency of various surfactants in the dedusting process.

Once the two parameters of the oil loss equation have been determined from experiments using a surfactant-demulsifier mixture, the equation appears to be able to predict oil losses for other surfactant-demulsifier mixtures, so long as other system variables are unchanged.

FLOC FORMATION AND CARRYUNDER

A portion of the sludge layer often falls through the bulk O/W interface and settles to the bottom of the water phase in the form of flocs. While experimental measurements of oil loss indicate no decrease in oil loss due to floc formation, the advantage that floc formation offers is that removal of the sludge layer by mechanical means becomes redundant. It

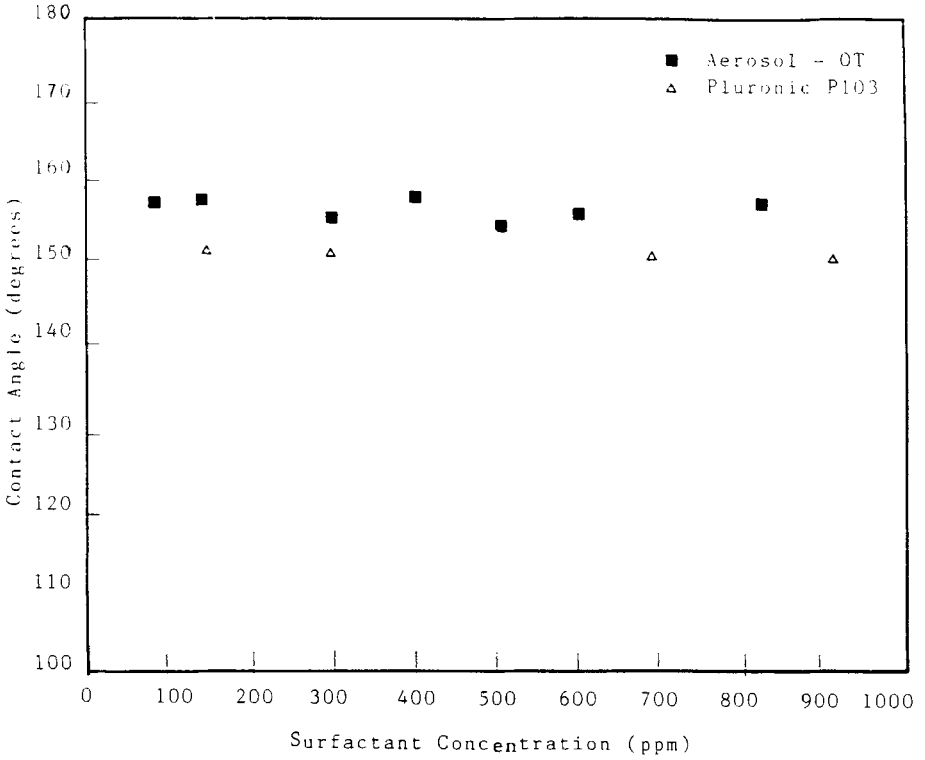

FIG. 10. Variation of contact angle with surfactant concentration.

is therefore of interest to find the conditions under which flocs of solid particles with entrained oil break through the bulk O/W interface and settle into the clear-water phase.

A force balance must be conducted on the floc at the O/W interface in order to find the equilibrium states at which the floc will stay at that interface. For a body that is irregularly shaped, such a force balance is not trivial. It is, therefore, necessary to assume the floc to be a spherical body of uniform contact angle and density. The force balance of a sphere at a planar O/W interface has been conducted by many workers, but the work of Rapachietta and Neumann (*4*) is perhaps the most complete since they include the deformation of the bulk interface (due to the presence of the sphere) by solving the Laplace equation for a deformed interface.

In this section a free-body force analysis is conducted on a spherical

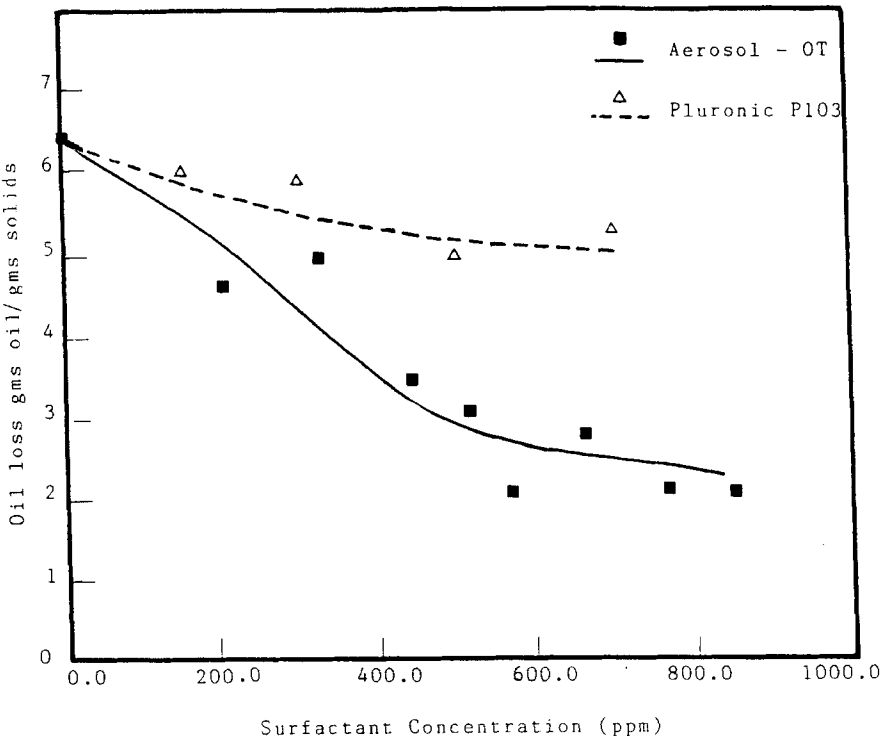

FIG. 11. Variation of oil loss with surfactant concentration.

floc at an O/W interface to find the equilibrium states at which the floc will reside at the interface. Since the size of the floc is related to the number of particles in the floc and the contact angle, the analysis can be related to both the previous sections through process variables that are common.

Experimental observations of the phenomenon of solids transfer and subsequent separation of the oil and water phases show that a part of the sludge layer decomposes into flocculates which then break through the bulk O/W interface and settle to the bottom of the water phase. A possible mechanism of floc formation and carryunder are discussed in this section. When more and more droplets of the solids-stabilized emulsion settle to the sludge layer, the force acting on the droplets in the bottom layer increases. The droplets of this layer get squeezed, resulting in their coalescence with each other and/or with the bulk O/W interface. The coalescence of a droplet with the bulk interface releases the water in the

droplet to the bulk-water phase. What remains is a mixture of solid particles and entrained oil associated with the droplet. This is called the floc. One can visualize the process of floc formation to include the following different cases:

a. Coalescence of one droplet with the bulk interface
b. Coalescence of two droplets with each other followed by coalescence with the bulk interface
c. Coalescence of three or more droplets with each other followed by coalescence with the bulk interface

In all the cases listed above, the ultimate coalescence of the droplet with the bulk-water phase is necessary since this is the only way the water in the droplet can be released to form a floc.

Once floc formation has occurred, it is necessary to find the conditions under which it will fall through the bulk O/W interface. A free-body force balance has hence to be written. If the net vertical force acting downward is positive, that body will fall through the interface.

The problem of a sphere at a flat O/W interface has been considered by a number of investigators. Scheludko and Nikolov (*6*) solved the force balance equation for a sphere suspended from a balance into a fluid interface. The expression for determining the liquid interfacial tension has been derived from the maximum force recorded over a number of immersion depths. Princen (*7*) formulated the force expression for a sphere at a fluid interface.

The most common problem associated with such a force analysis is that the force exerted by the deformed interface around the sphere can only be accurately known by solving the Laplace equation for the interface. Numerical solution of the three-dimensional Laplace equation has become possible only in the past few years. Rapachietta and Neumann (*4*) reported the numerical solution to the Laplace equation. They also proposed a semi-empirical equation for the deformation of the interface which can be used in lieu of the exact Laplace equation. In the discussion that ensues, this semi-empirical form of the Laplace equation has been used.

For a floc to settle through the O/W interface, its density must be larger than the densities of both oil and water. Even if it has a density larger than both phases, it may yet occupy an equilibrium position at the interface if the surface tension forces are sufficiently large. The following analysis investigates the forces acting on a floc at the interface. To make the problem mathematically tenable, certain assumptions have to be made. The floc that is formed due to the coalescence process of one or

more droplets with the O/W interface is assumed to be a rigid sphere of radius R_f and density ρ_f. It is assumed to have a finite contact angle θ measured through the water phase. The floc is further assumed to contain particles and entrapped oil, the latter being known from the geometric model for oil loss that was described in the previous section. Each solids-stabilized water droplet is assumed to contain spherical solid particles packed in a hexagonal close-packed arrangement on the droplet surface. The floc is assumed to be a free body at the interface, and the influence of neighboring droplets or flocs is neglected.

The radius of the floc is given by a volume balance on the coalescing droplets:

$$(4\pi/3)R_f^3 = (4\pi/3)R_p^3 N_p N_c[1 + V_{tot}(\rho_p/\rho_o)] \tag{23}$$

where N_c is the number of coalescing water droplets.

The values of N_p and V_{tot} are obtained for a particular size ratio by solving Eqs. (4), (9), (10), and (18). N_c is a parameter of the analysis and cannot be ascertained independently.

The density of the floc can be determined from a mass balance on the coalescing droplets:

$$R_f^3\rho_f = N_p N_c R_p^3 \rho_p[1 + V_{tot}(\rho_p/\rho_o)] \tag{24}$$

Once the floc density has been evaluated for a given set of conditions, it is important to find out if this density is greater than that of the two bulk phases. It is of interest to proceed with the analysis only if the value of ρ_f is larger than both ρ_w and ρ_o.

Figure 12 depicts a schematic of the stationary state of the floc at the fluid interface. The contact angle has been assumed to be equal to that of the solid particle. ϕ is the position parameter of the floc at the interface.

The net vertical force is obtained by the summation of the contributions of the surface tension force, the weight of the floc, and the vertical component of the hydrostatic pressure distribution around the floc (*4*). When this net force, acting downwards, is expressed in dimensionless form, it takes the following form:

$$G_{net} = 2\pi \sin\phi \sin(\theta + \phi) + 4\pi/3DC - (\pi/3)C(1 - \cos\phi)^2(2 + \cos\phi) + \pi Y_0 X_0 \sin\phi \tag{25}$$

where

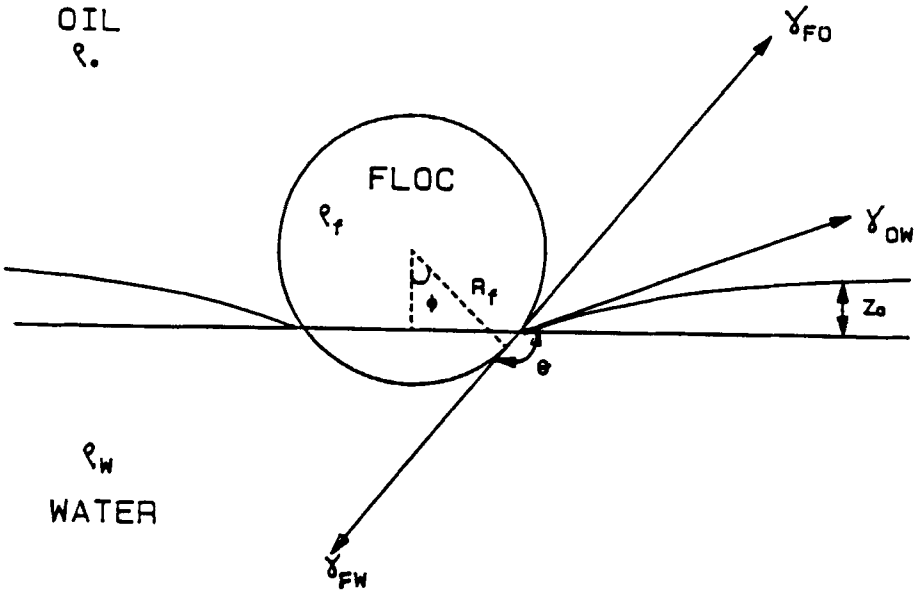

FIG. 12. Schematic of the stationary state of floc at an interface.

$$A^2 = \frac{(\rho_w - \rho_o)g}{\gamma_{ow}}$$

$$B = \frac{\pi(\rho_f - \rho_o)g}{\gamma_{ow}}$$

$$C = A^2 R_f^2$$

$$D = B/\pi A^2$$

$Y_0 = Z_0 A$ and $X_0 = C^{1/2} \sin \phi$.

Y_0 is the height of the deformed interface above the three-phase contact line. For a given set of values of ϕ, γ_{ow}, θ, and $\mathbf{n}$, it is possible to evaluate the net force acting on the floc, provided that the value of Y_0 is known. To estimate Y_0 precisely, it is necessary to solve the Laplace equation for the mathematically three-dimensional problem of the sphere at a fluid interface. Such a solution is numerically involved. Hence, an approximate equation for Y_0 that has been reported in the literature (*4*) was used:

$$\frac{1}{2}Y_0^2 - 1 - \frac{4}{X_0}\left[\left(1 - \frac{Y_0^2}{4}\right)^{3/2} - 1\right] + \cos(\theta + \phi - \pi) = 0 \quad (26)$$

This equation is implicit in Y_0 and was solved numerically using the Newton-Raphson technique.

In order to obtain the total force acting on a floc of given size, density, and contact angle, one needs to know the interfacial tension, θ, and Y_0. The O/W interfacial tension can be experimentally determined. In the previous section on oil loss modeling it was found that γ_{ow} is a simple function of the size of the water droplets that formed the sludge layer, provided other variables such as speed of agitation, impeller dimensions, etc. are kept constant. To compute numerical values of the total force on the floc, the following relationship between γ_{ow} and the size ratio was therefore used:

$$R_w/R_p = 20.2\gamma_{ow}^{0.44} \quad (27)$$

Equation (27) is valid only when the aforementioned conditions are met.

The position parameter ϕ can only be determined by experiment and in this analysis it has been retained as a parameter.

Figure 13 is a graphical representation of the calculation of G_{net} for the case of a floc formed by the coalescence of two solid stabilized droplets with each other and subsequently with the O/W interface ($N_c = 2.0$). The ratio of the water droplet size to the particle size was fixed at 10.0. Plots for five different values of the floc contact angle are shown in Fig. 13. A positive value of G_{net} implies that the floc will fall through the interface while a zero value implies that the floc will take up an equilibrium position at the interface. At a contact angle of zero (totally hydrophilic situation), no equilibrium state can exist at the interface and the floc will fall through the interface for all ϕ. As the floc becomes less hydrophilic, the range of values of ϕ for which the floc will fall decreases. For a contact angle of 150° (shale dust), all ϕ values less than 41° will cause the floc to fall through the interface. The force analysis also predicts the existence of two equilibrium states (when $G_{net} = 0.0$) for a spherical solid at the interface. The second equilibrium state is more easily discernible at low values of the drop to particle size ratio.

Since a specific system will have a spherical particle in equilibrium at the interface when the net force is zero, we can find the largest floc that can be supported at the interface by setting the force equation to zero. The resulting equation was solved simultaneously with the equation for

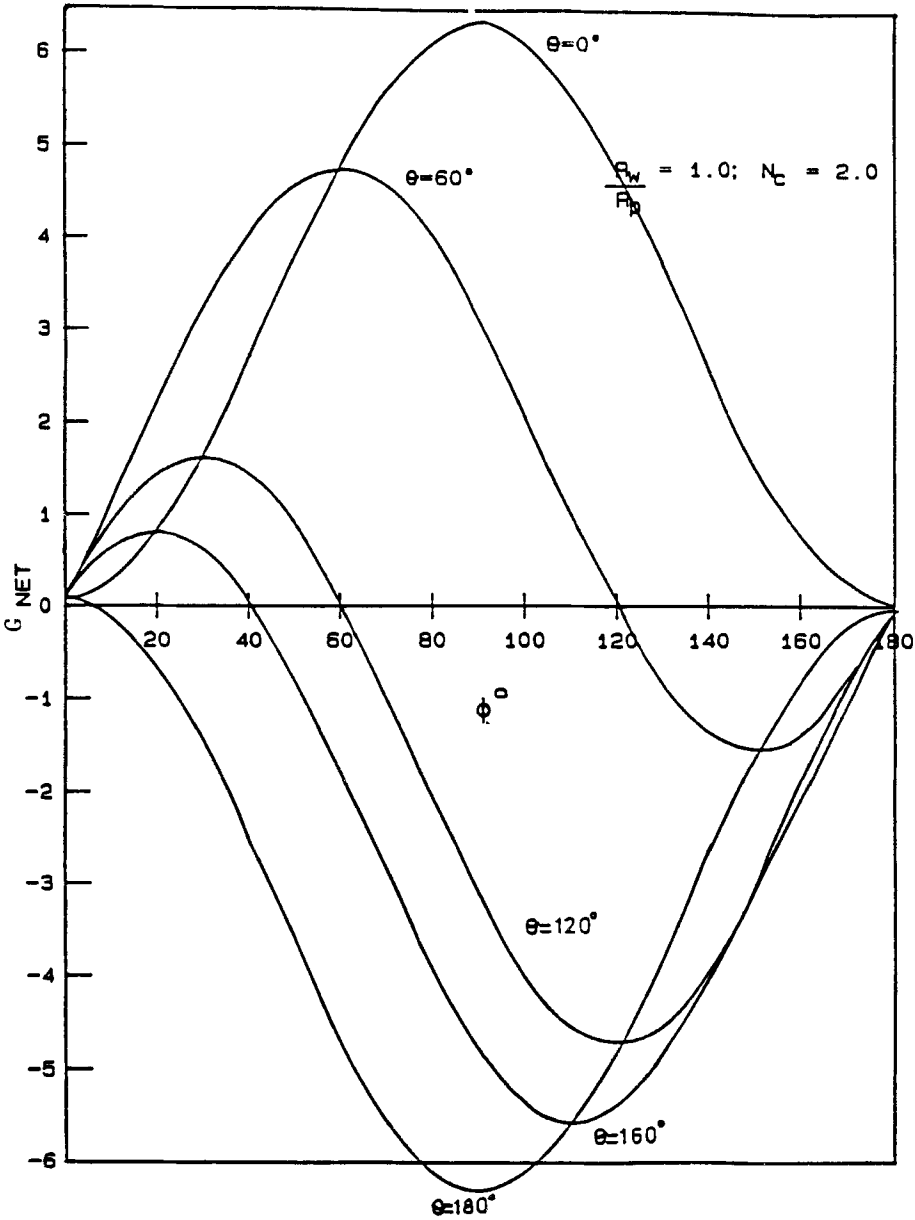

FIG. 13. Effect of location parameter (ϕ) and contact angle on the net force acting on the floc.

Y_0 by a Newton-Raphson scheme to obtain C for a fixed set of ϕ and θ. The results of this procedure, in graphical form, are shown in Fig. 14.

Figure 14 shows the influence of θ and ϕ on the size of the floc which allows for an equilibrium state, i.e., every point on the curves represents a possible equilibrium state. The points to the left of the maxima are the stable equilibrium states while those to the right are unstable equilibrium states. It should be noted that the term A in C is not a constant but varies as the drop size changes with interfacial tension. The maxima of the curves give the largest size of the floc that can be supported at the interface. Figure 14 illustrates that the critical radius decreases as the floc becomes more hydrophilic. Also, the maxima are shifted toward larger values of ϕ as θ decreases. Thus, if $\theta = 150°$ and $N_c = 1.0$, the maximum value of C is 0.61. If the O/W interfacial tension is 1.0 dyn/cm, the maximum floc radius of shale dust that can be supported at the interface is 513.3 μm. All flocs larger than this size will fall through the interface. In order to allow for smaller flocs to fall through the interface, it is necessary to decrease the contact angle or the interfacial tension. A decrease in the contact angle from 140 to 120° at an interfacial tension of 1 dyn/cm decreases the floc radius from 513.3 to 360.0 μm. Also, a decrease in the interfacial tension from 1.0 to 0.5 dyn/cm at a contact angle of 140° decreases the maximum permissible value of the floc radius from 513.3 to 363.0 μm.

The implication of the above analysis is that the manipulation of variables such as contact angle and interfacial tension can decrease the radius of the largest floc that can exist in equilibrium at the interface. Such a decrease would facilitate smaller flocs all falling from the sludge layer to the bottom of the bulk water phase. On the other hand, if the floc size can be determined *a priori* for a given set of conditions, the force analysis can predict if that floc will fall through the interface or not.

CONCLUSIONS

Free energy analysis revealed that the size ratio (**n**), contact angle, and number of particles per drop are important parameters for determining the ease of transfer of particles from oil to water, with transfer being favored at higher values of the size ratio **n**. Also, the range of permissible contact angles was found to increase with increasing values of **n**.

Oil loss analysis showed that the size ratio is once again critical to determining oil loss, with lower values of **n** favoring lower oil loss. The oil loss was not found to be strongly dependent on the contact angle. Both the free energy analysis as well as the oil loss model predict the

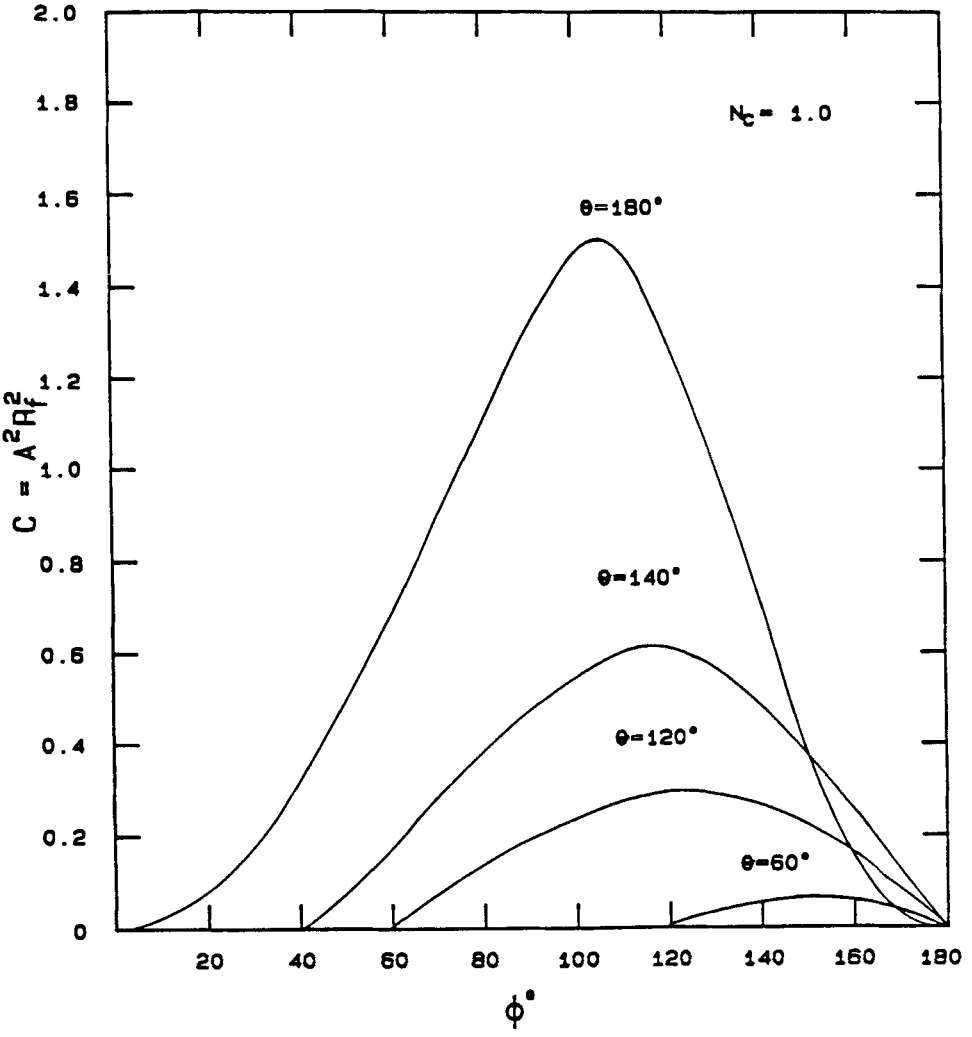

FIG. 14. Influence of θ and φ on the critical size of the floc at N_c = 1.0.

importance of the size ratio, but the former favors a large value of **n** while the latter recommends a small value of **n**. The size ratio therefore has to be optimized after taking into account all aspects of the process.

A semi-empirical equation was derived to express oil loss in terms of the interfacial tension and contact angle. Experiments revealed an excellent agreement between experimental values of oil loss and those predicted by the oil loss equation. Such an equation is very useful in assessing the effectiveness of various surfactants in decreasing oil loss, especially since the only inputs required are the interfacial tension and the contact angle, both of which are relatively easy to measure.

Free-body force analysis of floc stability at the interface identified the largest size of the floc that can be stabilized at the interface. This critical size could be decreased by either decreasing the contact angle or the O/W interfacial tension.

Acknowledgments

This study was supported by the Exxon Research and Engineering Company as part of their Frontiers of Separations Program. The discussions with Drs L. Kaye, D. L. Smith, R. Gupta, and E. C. Hsu are gratefully acknowledged.

REFERENCES

1. L. A. Kaye and R. J. Fiocco, *Sep. Sci. Technol., 19,* 783 (1985).
2. V. B. Menon, PhD Thesis, Illinois Institute of Technology, Chicago, Illinois, 1986.
3. M. T. Jacques, A. D. Hovarongkura, and J. D. Henry Jr., *AIChE J., 25,* 160 (1979).
4. A. V. Rapachietta and A. W. Neumann, *J. Colloid Interface Sci., 59,* 555 (1977).
5. S. Winitzer, *Sep. Sci., 8,* 45 (1973).
6. A. D. Scheludko and A. D. Nikolov, *J. Colloid Polym. Sci., 253,* 396 (1974).
7. H. M. Princen, in *Surface and Colloid Science,* Vol. 2 (E. Matijevic, ed.), Wiley, New York, 1969, pp. 1-84.

Received by editor December 1, 1986